Two-Photon-Induced versus One-Photon-Induced Isomerization Dynamics of a Bistable Azobenzene Derivative in Solution

ARTICLE *in* THE JOURNAL OF PHYSICAL CHEMISTRY B · AUGUST 2015

Impact Factor: 3.3 · DOI: 10.1021/acs.jpcb.5b07008 · Source: PubMed

8 AUTHORS, INCLUDING:

A. L. Dobryakov

Humboldt-Universität zu Berlin

72 PUBLICATIONS **866** CITATIONS

SEE PROFILE

Alexander A. Granovsky

Kintech Lab

79 PUBLICATIONS **643** CITATIONS

SEE PROFILE

Stefan Hecht

Humboldt-Universität zu Berlin

188 PUBLICATIONS **5,901** CITATIONS

SEE PROFILE

Sergey A Kovalenko

Humboldt-Universität zu Berlin

154 PUBLICATIONS **2,836** CITATIONS

SEE PROFILE

THE JOURNAL OF PHYSICAL CHEMISTRY B

Article

pubs.acs.org/JPCB

Two-Photon-Induced versus One-Photon-Induced Isomerization Dynamics of a Bistable Azobenzene Derivative in Solution

J. Moreno,[†] M. Gerecke,[†] A. L. Dobryakov,[†] I. N. Ioffe,[‡] A. A. Granovsky,[§] D. Bléger,[†] S. Hecht,*[,†] and S. A. Kovalenko*[,†]

[†]Department of Chemistry, Humboldt-Universität zu Berlin, Brook-Taylor-Strasse 2, 12489 Berlin, Germany

[‡]Department of Chemistry, Lomonosov Moscow State University, 119991 Moscow, Russia

[§]Firefly Project, 117593 Moscow, Russia

Supporting Information

ABSTRACT: We report on a bistable azobenzene derivative with sufficiently high 2-photon absorption to induce its photochemical isomerization and measurable excited state dynamics. Broadband transient absorption spectra were recorded and compared upon 1-photon (331 nm) and 2-photon (640 nm) excitation of the $S_0 \rightarrow S_2$ transition. The spectra are different at early ($t \sim 1$ ps) and late ($t \sim 100$ ps) time but show similar photoisomerization behavior on a 10 ps time scale. With 2-photon excitation, strong population transfer $S_2 \rightarrow S_n$ occurs due to resonance absorption of a third pump photon. Subsequent internal conversion $S_n \rightarrow S_1$ results in a very hot S_1 population causing extra-broadening of the transient spectra. The resonance pump absorption is common with nonlinear excitation and should be taken into account when considering photochemical applications. The 2-photon excitation cross-section $\sigma^{(2)}$ at 640 nm was measured to be 7 GM for the specific tetra-*ortho*-fluorinated azobenzene derivative and 1 GM for unsubstituted parent azobenzene. The direct 2-photon induced trans-to-cis isomerization, described herein, provides an unprecedented potential for spatially addressing P-type (bistable) azobenzene photoswitches in 3D.

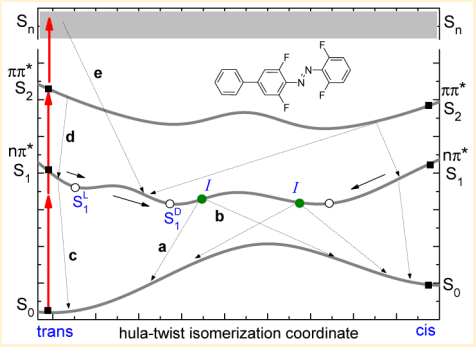

I. INTRODUCTION

Azobenzene (**AZ**) and derivatives constitute an important class of photoswitches which are capable to isomerize under strong constrains[1−3] as in solid matrixes or polymer chains rending these compounds promising for nanotechnological applications. The photophysics and photochemistry of **AZ** has been studied thoroughly.[4−10] Azobenzene absorption spectra (see Figure 1) include two types of transitions: a weak $n\pi^*(S_0 \rightarrow S_1)$ band centered at 440 nm, and a strong $\pi\pi^*(S_0 \rightarrow S_2)$ one at 320 nm. The isomerization yields for $n\pi^*$ and $\pi\pi^*$ excitation are different, in violation of Kasha's rule. This indicates a complex structure of potential energy surfaces with multiple conical intersections allowing for different excitation-dependent relaxation paths.[9]

We have recently reexamined[10] the photoisomerization dynamics of trans- and cis-azobenzene (*t***AZ** and *c***AZ**, respectively) with femtosecond broadband transient absorption and stimulated Raman spectroscopies. The results are summarized as follows. For *t***AZ** upon $n\pi^*$ excitation, excited wavepacket reaches (with 0.3 ps) a local minimum S_1^L, and over a barrier arrives (with 3 ps) at a dark intermediate S_1^D. From there isomerization ($S_1^D \rightarrow S_0$) occurs with 16 ps over a 12 kJ/mol barrier. Upon $\pi\pi^*$ excitation the wavepacket relaxes first to S_1 with 0.1 ps. Next, a part of population follows the described $S_1^L \rightarrow S_1^D \rightarrow S_0$ isomerization path, while the other experiences internal conversion (with 1.2 ps) to S_0 without isomerization. Independence of the kinetics on viscosity together with a long-lived intermediate suggest the hula-twist isomerization path,[11,9] consistent with isomerization under strong constrains.

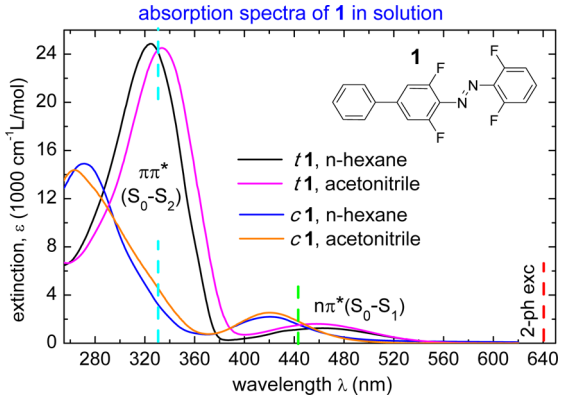

Figure 1. Trans (ε_t) and cis (ε_c) extinction spectra of **1** in solution. The $n\pi^*$ band is peaked at 460 nm for *t***1** and at 420 nm for *c***1**. The $\pi\pi^*$ band of *t***1** (about 320 nm) shifts by 840 cm^{-1} to the red when going from *n*-hexane to acetonitrile, indicating a much higher dipole moment μ_2 in S_2 compared to μ_0 in S_0. Excitation wavelengths (330, 442, and 640 nm) for transient absorption measurements are indicated by dashed lines.

Received: July 20, 2015
Revised: August 27, 2015
Published: August 31, 2015

DOI: 10.1021/acs.jpcb.5b07008
J. Phys. Chem. B 2015, 119, 12281−12288

In this paper, we report the isomerization dynamics of an azobenzene derivative upon 2-photon excitation. The 2-photon-induced isomerization[12,13] of a bistable (P-type) photoswitch is of great interest because of increased spatial resolution and more a transparent spectral window, despite a rather small 2-photon excitation cross-section.

II. EXPERIMENT

The setup has been described elsewhere.[14−16] Transient absorption (TA) spectra $\Delta A(\lambda,t)$are recorded at the magic angle, and for parallel $\Delta A_{\parallel}$ and perpendicular $\Delta A_{\perp}$ polarization, with time steps of 0.02, 0.2, and 2 ps. Measurements are performed in the range 275−690 nm with τ_{cc} = 0.09 ps (fwhm) instrument response, and timing precision of 0.02 ps over the full probe range. Multiple (12−32) pump−probe scans are used to improve the signal-to-noise. Transient anisotropy ρ is calculated as

$$\rho(\lambda, t) = (\Delta A_{\parallel} - \Delta A_{\perp})/(\Delta A_{\parallel} + 2\Delta A_{\perp}) = (\Delta A_{\parallel} - \Delta A_{\perp})/(3\Delta A)$$

A 10 mL solution of *t***1** (see molecular structure in Figure 1) is passed through a sample cell of l = 0.3 mm thickness. The peak of absorbance $A(\lambda)$ is adjusted to about 0.8 (corresponding to the sample concentration of 1.2 × 10^{-3} M) to ensure high quality signal in the bleach region. The pump and probe beams, with 15° between them, are focused onto the cell with spot diameter $a_P \approx$ 0.2 mm, $a_{pr} \approx$ 0.1 mm, respectively. The spots were measured by a microscope relative to a calibrated pinhole. The pump pulse energy E_P was measured with power meters (Spectra Physics or Thorlabs). For 1-photon excitation E_P was 0.3 μJ, and for 2-photon excitation E_P was in the range 4−10 μJ.

III. PROBE COMPOUND AND ITS ABSORPTION SPECTRA

The probe molecule, hereafter **1** (*t***1** for trans, *c***1** for cis) is depicted in Figure 1. Its synthesis is described.[17] The compound differs from parent **AZ** by fluorines at 2, 6 positions and by an additional aryl ring. The fluorines result in spectral separation of the *trans* and *cis* bands, a useful photoswitch property.[18] However, 2-photon absorption in the fluorinated **AZ** is symmetry forbidden ($\sigma^{(2)}$ = 0), therefore the aryl ring is added.

Absorption spectra in Figure 1 show the typical nπ^*($S_0 \rightarrow S_1$) band at 460 nm (*t***1**) or 420 nm (*c***1**), and the $\pi\pi^*$($S_0 \rightarrow S_2$) band about 320 nm (*t***1**) or 270 nm (*c***1**). Note a strong solvatochromic shift of the $\pi\pi^*$ band for *t***1**. This band in acetonitrile is red-shifted by 800 cm^{-1} relative to that in *n*-hexane. The shift $\Delta\nu_{abs}$ (cm^{-1}) can be estimated from dielectric continuum theory[19]

$$hc\Delta\nu_{abs} = \frac{g}{r^3}\mu_0(\mu_2 - \mu_0)$$

where g = 0.6 is the reaction field factor for acetonitrile, r is the molecular radius, and μ_0, μ_2 are permanent dipole moments in S_0, S_2. For r = 4 Å, μ_0 = 2 D, one estimates $\mu_2 \approx$ 10 D.

IV. QUANTUM CHEMICAL CALCULATIONS

The properties of **1** in the ground S_0 and excited S_1 and S_2 states were studied at the DFT/TDDFT level using the Firefly package[20] partly based on the GAMESS(US) source code[21] and Gaussian09.[22] The calculated parent *t***AZ** molecule is known to be planar in its S_0, S_1, and S_2 states.[10] However, fluorination of *t***1** leads to considerable repulsion between the electronegative fluorines and the lone nitrogen pairs. In S_0, PBE0/Def2-TZVP optimization result in rotation of the difluorophenyl rings by 29° relative to the planar C−N═N−C fragment, the angle between the biphenyl-bonded rings is 35°. For the cis isomer (*c***1**), the C−N═N−C fragment is nearly planar (the dihedral angle is ∼10°), but the N═N−C−Ph dihedral angles are as high as 59°. Nevertheless, *c***1** is only 0.35 eV less stable than *t***1**.

Table 1 presents TDDFT properties of the lowest excited states in *t***1** and *c***1** studied with PBE0 and CAM-B3LYP

Table 1. Excitation Energies E_{exc}, Oscillator Strengths f_{0j}, and Dipole Moments μ_i of 1 from (TD)DFT (Frozen Core)

	CAM-B3LYP/Def2-TZVP			PBE0/Def2-TZVP		
	E_{exc} (eV)	f_{0j}	μ_i (D)	E_{exc} (eV)	f_{0j}	μ_i (D)
trans S_0			0.9			1.0
trans S_1 (nπ^*)	2.57	0.06	0.4	2.42	0.07	0.3
trans S_2 ($\pi\pi^*$)	4.02	1.26	3.9	3.71	1.12	7.3
cis S_0			5.6			5.5
cis S_1 (nπ^*)	2.81	0.04	5.0	2.74	0.06	5.8
cis S_2 ($\pi\pi^*$)	4.42	0.34	10.3	3.95	0.19	9.5

exchange-correlation functionals. Like in **AZ**, S_1 and S_2 result from more or less pure nπ^* and $\pi\pi^*$ excitations, respectively. In the present case, the lack of molecular symmetry gives rise to Kohn−Sham HOMO and LUMO with mixed n and π character (see Supporting Information). Hence, in terms of Kohn−Sham orbitals, both vertical transitions formally include mixed HOMO−1 → LUMO and HOMO → LUMO contributions. CAM-B3LYP tends to yield more accurate excitation energy, especially for the more polar S_2 state where the dipole moment arises from partial charge transfer from the extra phenyl group.

Optimization of S_1 and S_2 gives ambiguous results depending on the xc functional employed. With CAM-B3LYP, we failed to locate any stationary points in both *t***1** and *c***1**. On the contrary, PBE0 predicts for *t***1** local minima in both S_1 and S_2 characterized by planarization of the azobenzene unit of *t***1**. Upon planarization, S_1 relaxes by 0.65 eV, the S_0−S_1 gap drops to 1.05 eV, and the transition strength becomes close to zero. The relaxation of S_2 is less pronounced; its energy drops by 0.43 eV and the S_0−S_2 gap drops to 3.02 eV.

The discrepancies between the results of CAM-B3LYP and PBE0 raise questions about the extent of the adequacy of the TDDFT when applied to such systems. On one hand, while planarization in S_1 rather expectable due to reduced F···N repulsion upon partial depopulation of the lone pairs and an increase in F···N distances, none of these effects applies in S_2. Thus, TD-PBE0 may be not accurate in description of the respective steric effects. On the other hand, prediction of a local minimum in S_1 by TD-PBE0 is more consistent with the experimental data than the results of TD-CAM-B3LYP. One might feel a need for further investigation of *t***1** and *c***1** with the use of post-HF methodology.

It is also instructive to compare the calculated 2-photon cross sections $\sigma^{(2)}$ in *t***1** and *t***AZ**. The $\sigma^{(2)}$ values were calculated using the sum-overstate approach basing on the 30 TD-PBE0 excited states. For *t***AZ**, $\sigma^{(2)}(S_0 \rightarrow S_2)$ = 0 by symmetry, while for *t***1** the calculated $\sigma^{(2)}(S_0 \rightarrow S_2)$ approached 3.6 GM. Thus, the calculations semiquantitatively reproduce $\sigma^{(2)}$ for *t***1** (see below) while the nonzero experimental value for *t***AZ** is possibly

DOI: 10.1021/acs.jpcb.5b07008
J. Phys. Chem. B 2015, 119, 12281−12288

due to vibronic effects. The $S_0 \rightarrow S_1$ transition is found to be nearly completely dark in 2-photon absorption for both *t*1 and *t*AZ.

V. PHOTOISOMERIZATION YIELDS

Trans-to-cis (Y_{tc}) and cis-to-trans (Y_{ct}) yields are determined by the actinometry method as described in the Supporting Information. The yields of **1** and of **AZ** are collected in Table 2. Of most interest is that for *t*1 under nπ^* or $\pi\pi^*$ excitation the yields are *the same*, while for *t*AZ they differ by a factor 2. Thus, Kasha's rule is restored for *t*1. Equal yields upon different excitations may correspond to similar excited-state evolutions.

Table 2. Photoisomerization Yields Y_{tc} and Y_{ct}

	nπ^*(S_0–S_1) 442 nm	$\pi\pi^*$(S_0–S_2) 330 nm
*t*1, *n*-hexane	0.15	0.16
*t*1, acetonitrile	0.16	0.16
*t*AZ, *n*-hexane[4,5]	0.24	0.12
*t*AZ, acetonitrile[4,5]	0.31	0.15
*c*1, *n*-hexane	0.28	0.09
*c*1, acetonitrile	0.37	0.10
*c*AZ, *n*-hexane[4,5]	0.55	0.31
*c*AZ, acetonitrile[4,5]	0.46	0.35

VI. EVOLUTION UNDER 1-PHOTON EXCITATION

TA spectra of *t*1 upon nπ^* excitation are shown in Figure 2. An early spectrum at t = 0.1 ps (black curve) reveals a bleach band around 330 nm, quite close to the $\pi\pi^*$ absorption peak in Figure 1, indicating that the bleach band is not strongly disturbed by ESA. The latter consists of two bands, ESA1 peaked at 380 nm and ESA2 at 540 nm. Within 1 ps (top panel), the ESA bands decay while the bleach remains nearly constant, reflecting an evolution in the S_1 state. After t = 1 ps (middle) the bleach recovers indicating $S_1 \rightarrow S_0$ isomerization or internal conversion. At 200 ps (bottom) the evolution is complete. The residual signal is due to *trans* and *cis* species in S_0, and the signal can be fitted with the difference extinction ($\varepsilon_c - \varepsilon_t$) (yellow curve). Deviations in acetonitrile suggest an additional photoproduct.

Signal evolutions (kinetics) are derived from band integrals[15]

$$I(\lambda_1, \lambda_2; t) = \frac{1}{\ln(\lambda_2/\lambda_1)} \int_{\lambda 1}^{\lambda 2} \Delta A(\lambda, t)\, d\lambda/\lambda$$

where λ_1, λ_2 indicate a spectral region of interest. Figure 3 shows the short-time behavior of the characteristic bands. ESA1 and ESA2 decay biexponentially (with 0.3 and 3 ps) whereas the bleach remains nearly constant on this time scale. This is a

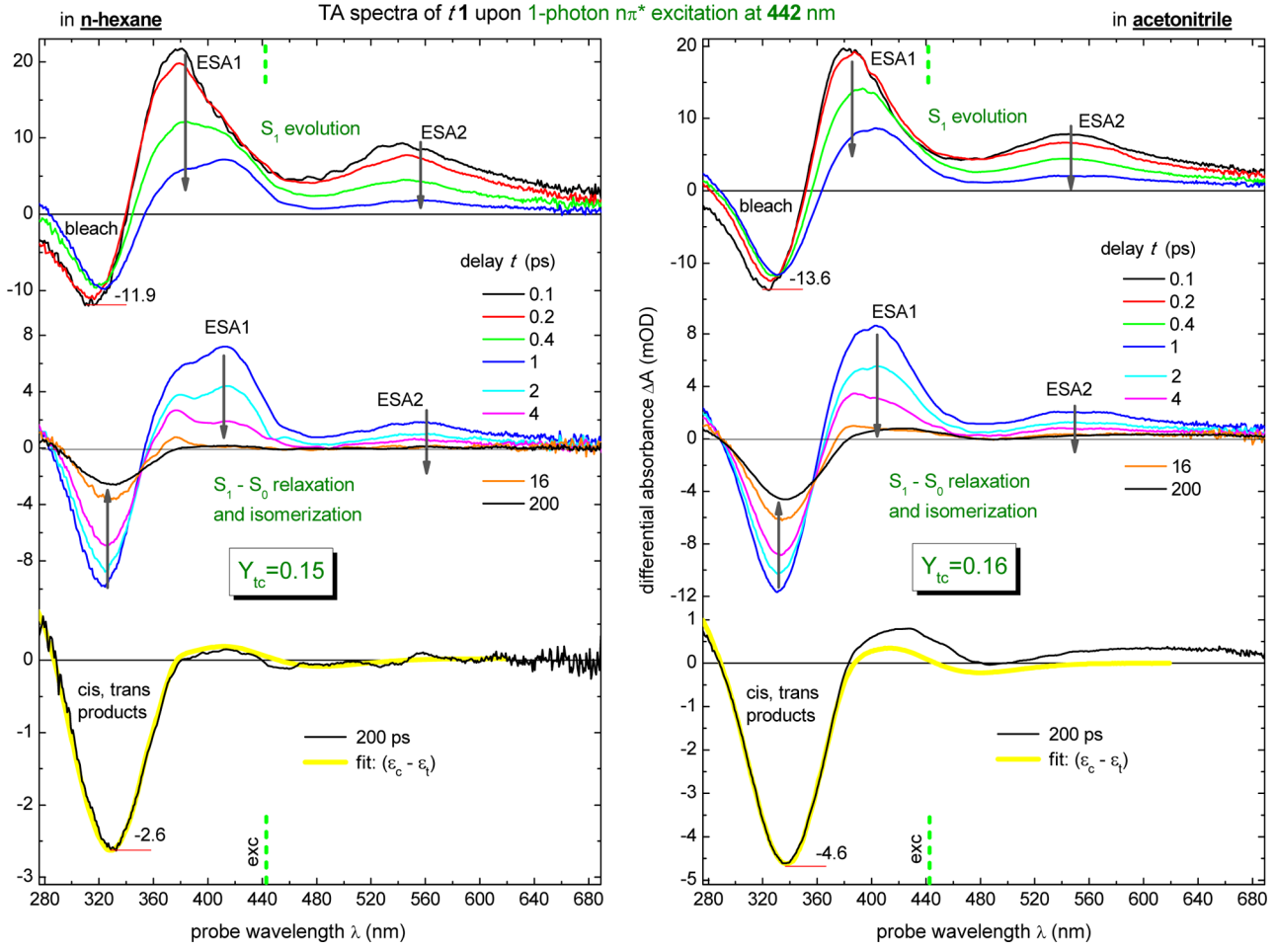

Figure 2. Transient absorption (TA) spectra of *t*1 in *n*-hexane (at left) and acetonitrile upon 1-photon nπ^*($S_0 \rightarrow S_1$) excitation at λ_P = 442 nm (E_P = 0.9 μJ, a_p = 200 μ, a_{pr} = 100 μ). For early, t = 0.1–1 ps, delays (top panels) the bleach stays nearly constant, while ESA bands (ESA1, ESA2) decay reflecting an S_1 evolution. After t = 1 ps (middle frames) the bleach recovery indicates $S_1 \rightarrow S_0$ relaxation and isomerization. At 200 ps, the evolution is complete. The residual spectrum (at the bottom) is due to mainly trans and cis S_0 species and can be fitted by their difference absorption ($\varepsilon_c - \varepsilon_t$). Deviations for acetonitrile indicate an additional product.

DOI: 10.1021/acs.jpcb.5b07008
J. Phys. Chem. B 2015, 119, 12281–12288

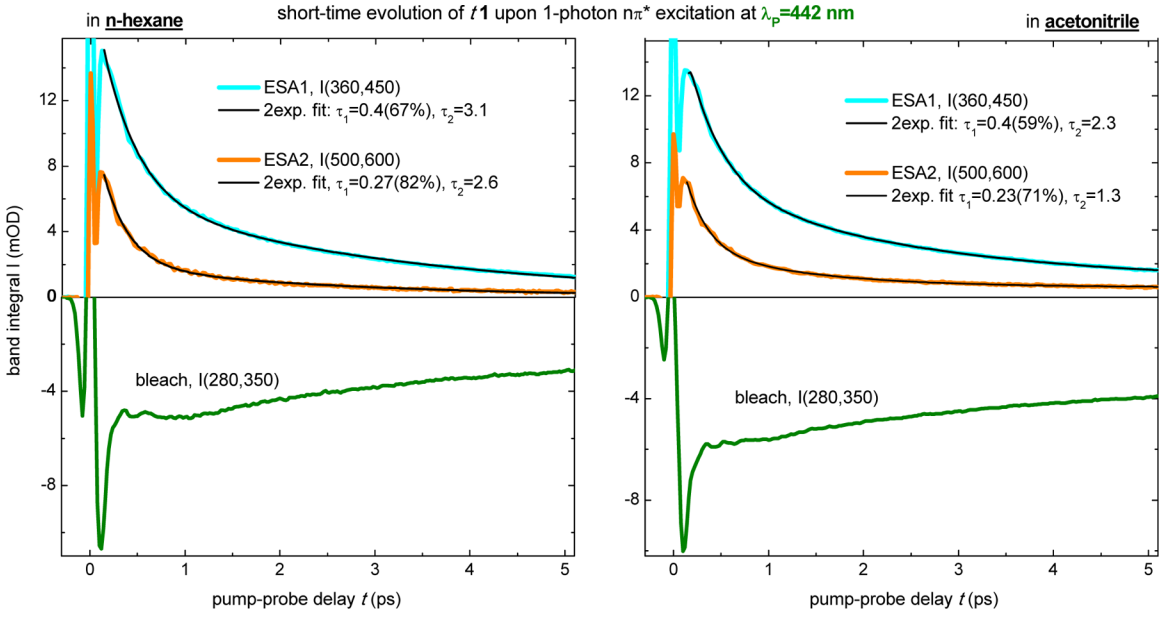

Figure 3. Short-time kinetics upon 1-photon $n\pi^*(S_0 \rightarrow S_1)$ excitation at 442 nm from band integrals $I(\lambda_1,\lambda_2,t)$. ESA bands decay biexponentially, $a_1 \exp(-t/\tau_1) + a_2 \exp(-t/\tau_2)$, as indicated by inserts. A strong time-zero signal is due to solvent and coherent contributions, therefore fits start from t = 0.1 ps. The bleach signal decays much slower than ESA indicating an evolution in S_1. Generally the behavior is very similar to that of parent **AZ**. The fastest component, τ_1 = 0.2−0.4 ps, reflects barrierless relaxation to a local minimum S_1^L, while the slower one, τ_2 = 2−3 ps, corresponds to further $S_1^L \rightarrow S_1^D$ transition to a dark state S_1^D.

clear indication of a process in S_1. Noteworthy, the transient spectra and kinetics closely reproduce those of parent **AZ**, implying similar underlying processes. Namely, the short component should reflect a barrierless motion of excited wavepacket, from the Franck−Condon region to a local minimum S_1^L, while the 3 ps component corresponds to further motion over a barrier relaxing to a dark intermediate S_1^D.

Next, consider the *t***1** TA spectra upon 1-photon $\pi\pi^*$ ($S_0 \rightarrow S_2$) excitation, as shown by two upper panels of Figure 4. Here a new ESA3 ($S_2 \rightarrow S_n$) band appears around 600 nm at t = 0.1 ps (black curve). A fast ∼0.1 ps decay of this band reflects $S_2 \rightarrow S_1$ internal conversion. At t > 1 ps (middle panel) the evolution proceeds similar to that under $n\pi^*$ excitation, as evident from comparison of Figures 4 and 2.

Long-time bleach recoveries upon $n\pi^*$ and $\pi\pi^*$ excitation (1-photon) are shown in the upper panels of Figure 5. Both kinetics are biexponential with similar fast τ_1 = 2−3 ps and slow τ_2 = 12−13 ps decay components. The former corresponds to internal conversion to S_0 (without isomerization), while the latter reflects isomerization from the intermediate S_1^D. Recall that for *t***AZ** internal conversion is *absent* under $n\pi^*$ but present upon $\pi\pi^*$ excitation, whereas for *t***1** the conversion takes place with both excitations. Fit parameters for the bleach kinetics are collected in Table 3 together with molecular rotational diffusion times.

VII. EVOLUTION UNDER 2-PHOTON EXCITATION

TA spectra after 2-photon $\pi\pi^*$ excitation at 640 nm (E_P = 11 μJ, a_p = 0.2 mm) are displayed at the bottom of Figure 4. The spectra start at t = 0.4 ps when intense solvent and coherent contributions disappear. Also, the probe region around 640 nm suffers from strong scattering of the pump. Despite the excitation is within the $\pi\pi^*(S_0 \rightarrow S_2)$ band, transient ESA spectra differ from those after 1-photon excitation (upper panels). In particular, at $t \sim$ 1 ps the ESA1 and ESA2 bands are not resolved anymore, and at late time additional products are seen about 440 nm. These features are explained as follows. The pump at 640 nm (red dashed line) is in resonance with ESA3 corresponding to a $S_2 \rightarrow S_n$ transition. Therefore, a substantial part of the S_2 population (created by 2-photon excitation) is transferred higher up to S_n by resonance absorption of a third pump photon.[23] Subsequent internal conversion back to S_1 (with ∼1 ps)[23] results in a very hot S_1 population that causes extra-broadening of the ESA bands.

What part of the initial S_2 population may be transferred to S_n? This can be estimated with the saturation parameter $J_P\sigma_{640}$. Here $J_P = E_P/(h\nu_P a_P^2) = 8.9 \times 10^{16}$ cm^{-2} is the surface density of the pump photons, σ_{640} is the absorption cross-section at 640 nm via ESA3, and $\sigma = 3.82 \times 10^{-21}\varepsilon$. Comparing ESA3 with the bleach (Figure 4, top left), one estimates $\sigma_{640} \approx \sigma_{320}/3 = 3.1 \times 10^{-17}$ cm^2 that gives

$$J_P\sigma_{640} \approx 3 \quad (1)$$

Thus, about 2/3 of the 2-photon-excited S_2 population is transferred higher up to S_n because of resonance with the ESA3 band. The population returns back to S_1 within 1 ps resulting in a very hot state. Nonetheless, the high S_1 temperature has no effect on the bleach recovery time, which remains 13−14 ps, just as for 1-photon excitation. This is clear from Table 3, and from Figure 5 where 2-photon bleach kinetics are shown at the bottom. Moreover, the fast τ_1 recovery is absent (in *n*-hexane) or strongly suppressed (in acetonitrile), very similar as for **AZ** under $n\pi^*$ excitation (see Table 3). We come back to this point in the Discussion.

Figure 6 compares bleach anisotropy decays upon 1- and 2-photon excitation. Initial anisotropy $\rho(0)$ = 0.4 is expected for 1-photon excitation, and $\rho(0)$ = 0.57 should be for 2-photon excitation,[24] in good agreement with the data.

To ensure that isomerization products arise from 2-photon excitation we performed the following experiment. A 50 μL solution of *t***1** in *n*-hexane was illuminated at 640 nm, E_P = 20 μJ, with two passes in a 10 mm cell, at a 0.6 mm beam.

DOI: 10.1021/acs.jpcb.5b07008
J. Phys. Chem. B 2015, 119, 12281−12288

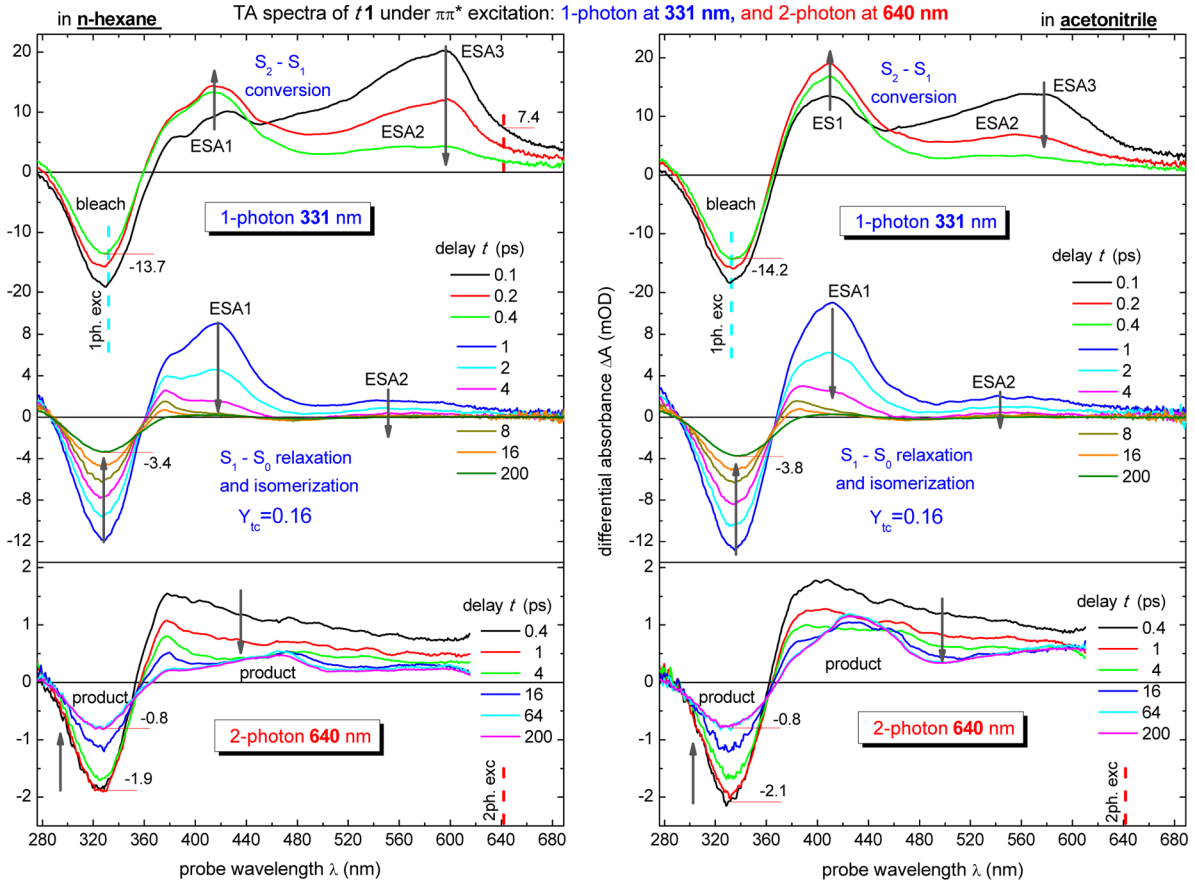

Figure 4. TA spectra of *t*1 in *n*-hexane and acetonitrile upon $\pi\pi^*(S_0 \rightarrow S_2)$ excitation: 1-photon at 331 nm (E_P = 0.3 μJ, a_p = 200 μ) or 2-photon at 640 nm (E_P = 11 μJ, a_p = 200 μ). 1-photon excitation reveals a new ESA3 band (corresponding to an $S_2 \rightarrow S_n$ transition) seen at t = 0.1 ps (black spectra on top). Subsequent ultrafast internal conversion to S_1 (with 0.1 ps) is followed by isomerization (middle), similar as for nπ^* excitation (compare to Figure 2). After 2-photon excitation (bottom frames), early ESA spectra are extra-broadened (ESA1 and ESA2 are not resolved) and photoproducts are seen at 440 nm. These features are due to $S_2 \rightarrow S_n$ population transfer and subsequent $S_n \rightarrow S_1$ internal conversion, resulting in a very hot S_1 population. The initial (2-photon-induced) S_2 population is efficiently transferred to S_n by resonance absorption (via ESA3) of a third pump photon.

The results are presented in Figure 7. The top frame shows the amount of *t*1 and *c*1 (measured with UPLC) as a function of illumination time. The bottom frame displays the power dependence of the isomerization rate. The slope 1.77 ± 0.37 confirms the 2-photon origin of the isomerization products.

VIII. EXCITATION CROSS-SECTION FROM BLEACH SIGNAL

The 2-photon excitation cross-section $\sigma^{(2)}$is obtained from the initial bleach $\Delta A_{bl}(0)$[23]

$$\sigma^{(2)}_{640} = \frac{2\tau_p \Delta A^{(2)}_{bl}(0)}{J_p{}^2 A} \tag{2}$$

Although $\Delta A^{(2)}_{bl}(0)$ is *a priori* not known because of overlap with unknown ESA, in some cases it can be estimated reasonably well. For example for 1-photon excitation, $\Delta A_{bl}(0)$ can be restored from late bleach $\Delta A_{bl}(\infty)$ as

$$\frac{\Delta A_{bl}(\lambda, \infty)}{\Delta A_{bl}(\lambda, 0)} = \Upsilon_{tc}[1 - \varepsilon_c(\lambda)/\varepsilon_t(\lambda)] \tag{3}$$

By using Figure 4 for $\pi\pi^*$ excitation in *n*-hexane, one has $\Delta A_{bl}(\infty)$ = −0.0034 at λ = 325 nm, Υ_{tc} = 0.16 (middle frame) and $\varepsilon_c/\varepsilon_t$ = 0.17, giving $\Delta A_{bl}(0)$ = −0.0253. Next $\Delta A_{bl}(0)/\Delta A_{bl}(0.4)$ = 1.85 (green spectrum at t = 0.4 ps, top left). Assuming the same ratio for 2-photon excitation (where spectra just start at t = 0.4 ps, Figure 4 bottom left) one gets $\Delta A^{(2)}_{bl}(0)$ = −0.0035. Then with τ_P = 0.08 ps, A = 0.82 one obtains $\sigma^{(2)}$ = 7.1 × 10^{-50} cm^{4}s = 7.1 GM. This value can be compared to a theoretical estimate[23]

$$\sigma^{(2)} = \frac{9.6\pi^3 \mu_{02}^2 (\Delta\mu)^2}{c^2 h^2 \Gamma} = 12 \text{ GM} \tag{4}$$

with μ_{02} = 5.5 D, $\Delta\mu = (\mu_2 - \mu_0)$ = 8 D, and Γ = 1.2 × 10^{14} s^{-1}. We measured also the 2-photon bleach signal from **AZ** at the same conditions (see Supporting Information) to estimate $\sigma^{(2)}_{AZ} \approx 1$ GM.

Also note that the photostationary state (PSS) reached by 2-photon excitation differs from that upon 1-photon excitation (see Supporting Information).

IX. DISCUSSION

Figure 8 summarizes our results. Here potential energy surfaces of **1** in solution are sketched as a function of the hula-twist coordinate, and relaxation/isomerization paths are shown by dashed arrows. Upon 1-photon nπ^* excitation of *t*1, population moves with 0.3 ps to a local minimum S_1^L and then overcomes a barrier to reach a dark intermediate S_1^D with 3 ps. From there

DOI: 10.1021/acs.jpcb.5b07008
J. Phys. Chem. B 2015, 119, 12281−12288

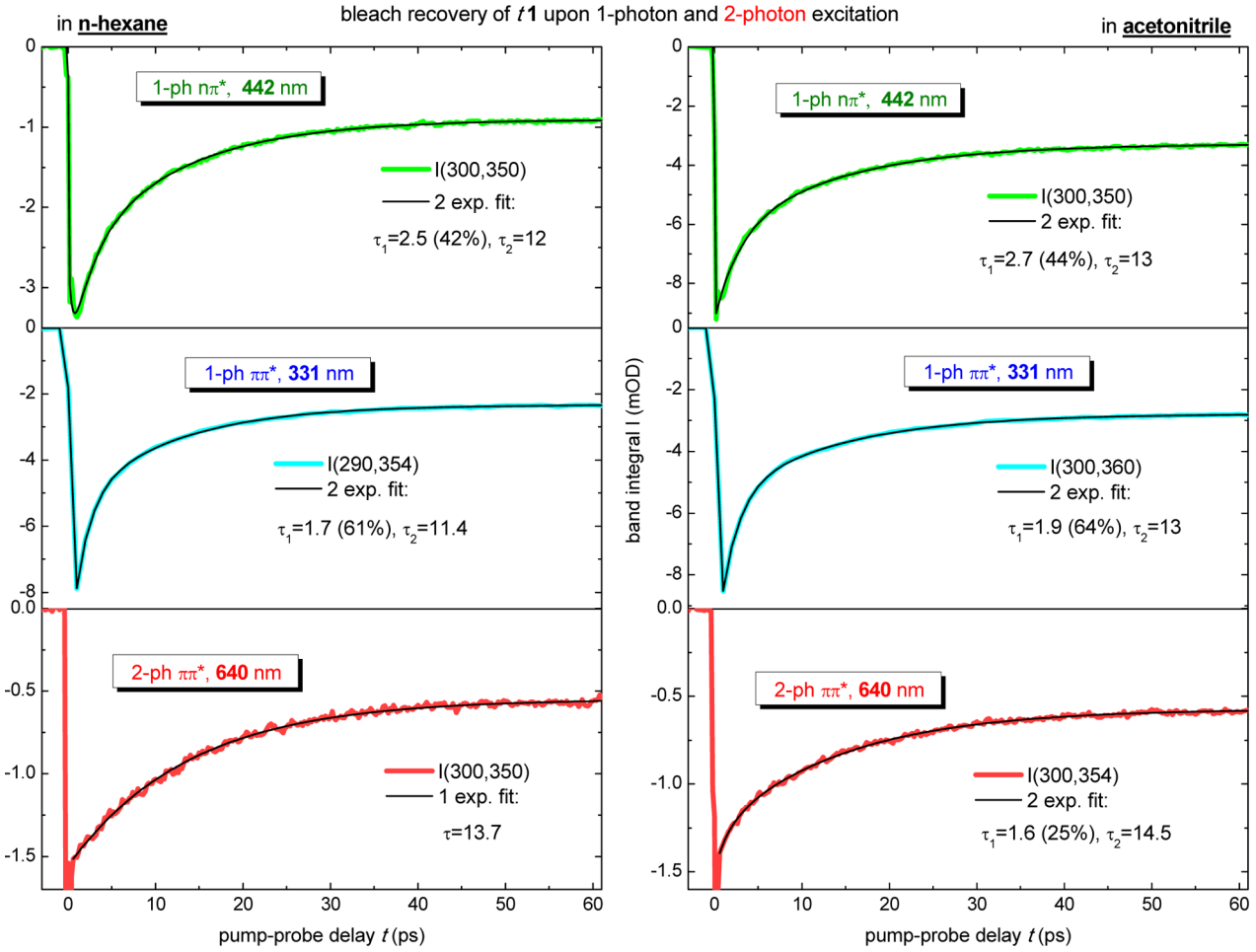

Figure 5. Bleach recovery kinetics of *t***1**. Upon 1-photon nπ* (top) or ππ* excitation (middle) the recovery is biexponential $a_1 \exp(-t/\tau_1) + a_2 \exp(-t/\tau_2)$. The fast τ_1 = 1.7−2.7 ps component reflects internal conversion to S_0 without isomerization, while the slow one (τ_2 = 12−13 ps) corresponds to $S_1^D \rightarrow S_0$ isomerization from S_1^D, similar as in the parent **AZ** molecule. Upon 2-photon excitation (bottom) the fast τ_1 component is absent or strongly suppressed, and the slow component is very similar to that under 1-photon excitation. The latter suggests that the 2-photon-induced isomerization also occurs from S_1^D, and on the same time scale as for 1-photon excitation.

Table 3. Bleach Recovery and Rotational Diffusion Times

		bleach recovery times (ps) and amplitudes		
	rotational diffusion time (ps) τ_R	1-ph. nπ* exc. 442 nm	1-ph. ππ* exc. 331 nm	2-ph. ππ* exc. 640 nm
*t***1**, *n*-hexane	47	2 exp. 2.5 (42%), 12 (58%)	2 exp. 1.7 (61%), 11.4 (39%)	1 exp. 14
*t***1**, acetonitrile	54	2 exp. 2.7 (44%), 13 (56%)	2 exp. 1.9 (64%), 13 (36%)	2 exp. 1.6 (25%), 14.5 (75%)
*t***AZ**, *n*-hexane	18	1 exp. 14	2 exp. 1.0 (35%), 14 (65%)	
*t***AZ**, acetonitrile	21	1 exp. 16	2 exp. 1.2 (35%), 17 (65%)	

isomerization occurs along arrows **a**, **b** with τ_2 = 12 ps, via conical intersection *I* over an 10 kJ/mol barrier. A part of the population reaches S_0 earlier by arrow **c** with τ_1 = 2.5 ps, without isomerization. Upon 1-photon ππ* excitation of *t***1**, the population created in S_2 relaxes to S_1 by internal conversion within 0.1 ps (arrow **d**). After that the molecule follows the same relaxation path as for nπ*excitation.

The observed evolution is qualitatively and quantitatively very similar to that of **AZ**, as seen from the fit parameters in Table 3. The only difference is that in **1** the fast τ_1 conversion (arrow **c**) is operative boh for nπ* and ππ* excitation, while in **AZ** the conversion is present for ππ* but absent for nπ* excitation. This difference in the kinetics correlates well with isomerization yields. For **AZ** the yield Y_{tc} drops down from 0.24 to 0.12 (twice) when switching from nπ* to ππ* excitation, whereas for **1** Y_{tc} = 0.15 remains the same for the both excitations.

2-photon excitation of *t***1** (red arrows) populates S_2 and simultaneously higher S_n states because of sequential reabsorption $S_2 \rightarrow S_n$ of the pump. Subsequent internal conversion $S_n \rightarrow S_1$ (∼1 ps) results in a very hot S_1 population. This internal conversion possibly populates directly S_1^D(along arrow **e**) that may explain the absence of a short component (represented by arrow **c**) in the bleach kinetics.

Despite strong excited-state absorption of the pump, the bleach signal and the isomerization products remain to be of 2-photon origin. This follows from bleach anisotropy data and from pump power dependence of the isomerization kinetics. At the same time ESA and stimulated emission (fluorescence) are of higher nonlinearity because of the third photon absorption.

DOI: 10.1021/acs.jpcb.5b07008
J. Phys. Chem. B 2015, 119, 12281−12288

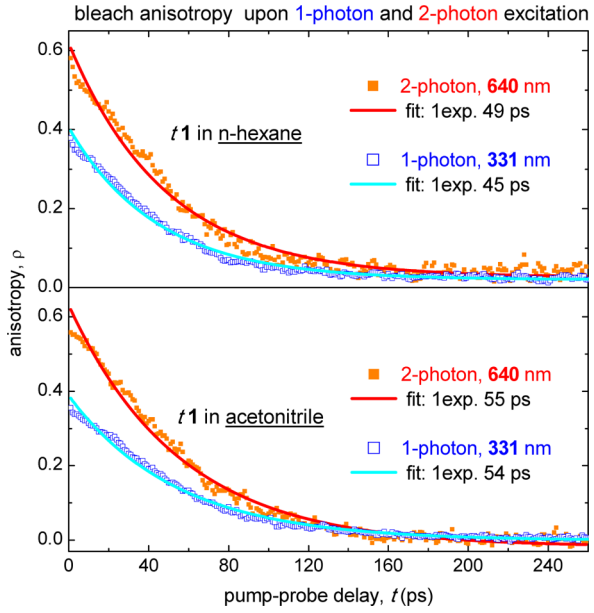

Figure 6. Bleach anisotropy $\rho(t)$ decay upon 1-photon (331 nm) and 2-photon (640 nm) excitation. Initial $\rho(0) = 0.4$ is expected for 1-photon excitation, and $\rho(0) = 0.6$ for 2-photon excitation. A monoexponential fit gives rotational diffusion times, $\tau_{rot} = 47$ ps in *n*-hexane and 55 ps in acetonitrile.

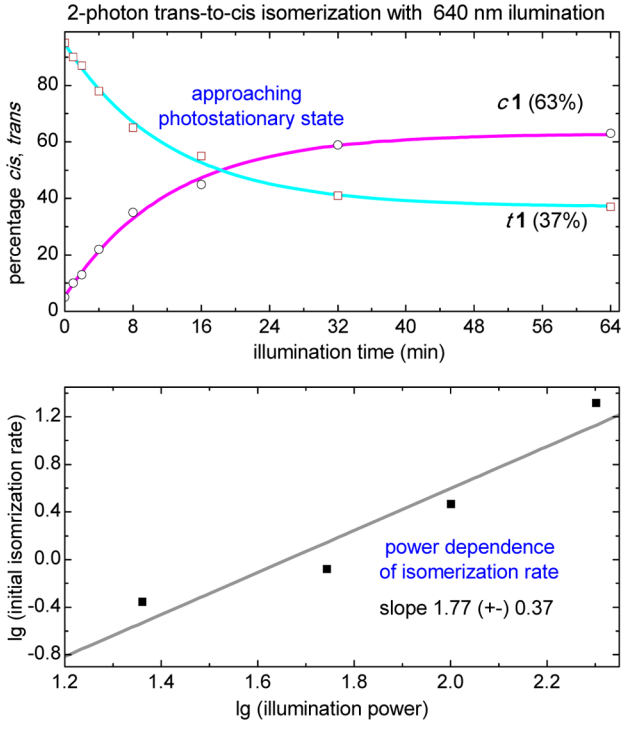

Figure 7. 2-photon-induced isomerization and photostationary state (PSS). A 50 μL solution of *t***1** in *n*-hexane is illuminated at 640 nm (E_P = 20 μJ, beam diameter 0.6 mm, with two passes through a 10 mm cell). Top graph shows the amounts of trans (cyan) and cis (magenta) isomers measured with UPLC. Bottom panel displays the power dependence of the isomerization rate. The slope 1.77 ± 0.37 agrees with the 2-photon-induced isomerization.

The latter is clearly an unwanted effect, which is however difficult to avoid. This is because ESA is usually red-shifted relative to the ground-state absorption. Nonetheless, it may be possible to reduce the effect by choosing an optimal excitation wavelength. In the present case, for example, excitation at 720 nm is preferable, as it decreases pump reabsorption while still remaining within the $\pi\pi^*$ band.

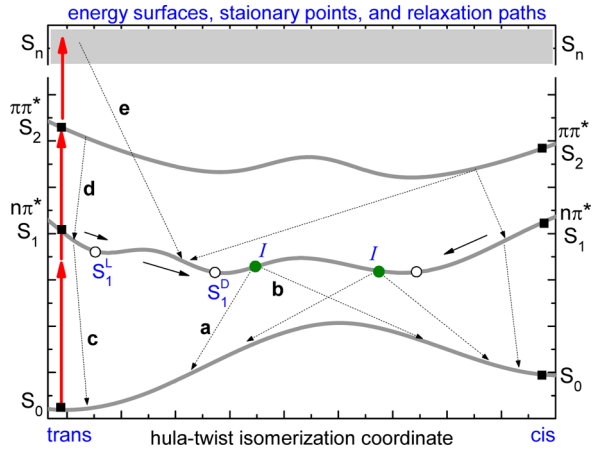

Figure 8. Potential energy surfaces of **1** along the hula−twist isomerization coordinate. Relaxation paths (dashed arrows) start from conical intersections *I* (closed circles) but only a few of them can be visualized in the one-dimensional graph. Squares mark wavepacket position upon vertical excitation, while open circles denote stationary points. Upon 1-photon $n\pi^*$ excitation, *t***1** population moves (with 0.3 ps) to a local minimum S_1^L, and over a barrier reaches (with 3 ps) a dark intermediate S_1^D, from where relaxation/isomerization occurs along arrows **a**, **b**, with $\tau_2 = 12$ ps over an 10 kJ/mol barrier. A part of the population reaches S_0 by arrow **c** with $\tau_1 = 2.5$ ps without isomerization. After 1-photon $\pi\pi^*$ excitation, $S_2 \rightarrow S_1$ conversion with 0.1 ps occurs first (arrow **d**) followed by the same relaxation path as upon $n\pi^*$excitation. 2-photon excitation (red arrows) populates S_2 and simultaneously higher S_n because of resonance $S_2 \rightarrow S_n$ pump absorption. Subsequent $S_n \rightarrow S_1$ internal conversion (with ∼1 ps) results in a very hot S_1 population. This conversion may proceed along arrow **e** directly to S_1^D, thus explaining the absence of a fast component (along arrow **c**) in the bleach kinetics.

An interesting point is why the isomerization rate $1/\tau_2$ is not affected by high temperature of the S_1 population. One possible mechanism[25,26] related to solute−solvent collisional activation has been discussed in connection with isomerization rates $1/\tau_{iso}$ of *trans*-stilbene. Its fluorescence yield γ in solution is independent of the excitation wavelength; and since $\gamma \sim \tau_{iso}$ the same is valid for τ_{iso}. In other words, the rate $1/\tau_{iso}$ is unaffected by intramolecular energy, or temperature. At the same time, *solvent* temperature strongly influences the isomerization rates of *trans*-stilbene. It may be possible that a similar collisional activation[26,27] is operative for azobenzenes as well.

In conclusion, we have studied 2-photon-induced isomerization of an azobenzene derivative. Bleach spectra and isomerization products are proved to be of the 2-photon origin while excited spectra are strongly affected by pump reabsorption. The 2-photon excitation cross-section was measured to be $\sigma^{(2)} = 7.1$ GM for the (P-type) tetrafluoroazobenzene derivative, and 1 GM for (T-type) parent azobenzene.

■ ASSOCIATED CONTENT

Supporting Information

The Supporting Information is available free of charge on the ACS Publications website at DOI: 10.1021/acs.jpcb.5b07008.

Cis transient spectra upon $n\pi^*$ and $\pi\pi^*$ excitation, UPLC spectra, photoisomerization yields, and PSS data from 1- and 2-photon excitation (PDF)

DOI: 10.1021/acs.jpcb.5b07008
J. Phys. Chem. B 2015, 119, 12281−12288

AUTHOR INFORMATION

Corresponding Authors

*(S.H.) E-mail: sh@chemie.hu-berlin.de.

*(S.A.K.) E-mail: skovale@chemie.hu-berlin.de.

Notes

The authors declare no competing financial interest.

ACKNOWLEDGMENTS

We are grateful to Prof. N. P. Ernsting for support and critical comments. Generous support by the Deutsche Forschungsgemeinschaft through SFB 658 and 1078, and the European Research Council through ERC-2012-STG_308117 are gratefully acknowledged. A.A.G. thanks the Russian Foundation of Basic Research (Grant No. 14-03-00887) for financial support. BASF AG, Bayer Industry Services, and Sasol Germany are thanked for generous donations of chemicals. I.N.I. and A.A.G. are thankful for the computational support by the Supercomputing Center of the Lomonosov Moscow State University[27]

REFERENCES

(1) Rau, H. Photoisomerization of Azobenzenes. In *Photoreactive Organic Thin Films*; Sekkat, Z., Knoll, W., Eds.; Elsevier Science: Dordrecht, The Netherlands, 2002.

(2) Yager, K. G.; Barrett, C. J. Novel Photo-Switching Using Azobenzene Functional Materials. *J. Photochem. Photobiol., A* **2006**, *182*, 250−261.

(3) Khan, A.; Kaiser, C.; Hecht, S. Prototype of a Photoswitchable Foldamer. *Angew. Chem., Int. Ed.* **2006**, *45*, 1878−1881.

(4) Bortolus, P.; Monti, S. Cis-Trans Photoisomerization of Azobenzene. Solvent and Triplet Donors Effects. *J. Phys. Chem.* **1979**, *83*, 648−652.

(5) Siampiringue, N.; Guyot, G.; Monti, S.; Bortolus, P. The Cis-Trans Photoisomerization of Azobenzene: An Experimental Reexamination. *J. Photochem.* **1987**, *37*, 185−188.

(6) Lednev, I. K.; Ye, T.-Q.; Hester, R. E.; Moore, J. N. Femtosecond Time-Resolved UV-Visible Absorption Spectroscopy of Trans-Azobenzene in Solution. *J. Phys. Chem.* **1996**, *100*, 13338−13341.

(7) Satzger, H.; Spörlein, S.; Root, C.; Wachtveitl, J.; Zinth, W.; Gilch, P. Fluorescence Spectra of Trans- and Cis-Azobenzene-Emission from the Frank-Condon State. *Chem. Phys. Lett.* **2003**, *372*, 216−223.

(8) Satzger, H.; Root, C.; Braun, M. Excited-State Dynamics of Trans- and Cis-Azobenzene after UV Excitation in the $\pi\pi^*$ Band. *J. Phys. Chem. A* **2004**, *108*, 6265−6271.

(9) Böckmann, M.; Doltsinis, N. L.; Marx, D. Nonadiabatic Hybrid Quantum and Molecular Mechanic Simulations of Azobenzene Photoswitching in Bulk Liquid Environment. *J. Phys. Chem. A* **2010**, *114*, 745−754.

(10) Quick, M.; Dobryakov, A. L.; Gerecke, M.; Richter, C.; Berndt, F.; Ioffe, I. N.; Granovsky, A. A.; Mahrwald, R.; Ernsting, N. P.; Kovalenko, S. A. Photisomerization Dynamics and Pathways of trans- and cis-Azobenzene in Solution from Broadband Femtosecond Spectroscopies and Calculations. *J. Phys. Chem. B* **2014**, *118*, 8756−71.

(11) Liu, R. S. H.; Asato, A. E. The Primary Process of Vision and the Structure of Bathorhodopsin: A Mechanism for Photoisomerization of Polyenes. *Proc. Natl. Acad. Sci. U. S. A.* **1985**, *82*, 259−263.

(12) Magennis, S. W.; Mackay, F. S.; Jones, A. C.; Tait, K. M.; Sadler, P. Two-Photon-Induced Photoisomerization of an Azo Dye. *Chem. Mater.* **2005**, *17*, 2059−2062.

(13) Houk, A. L.; Zheldakov, I. L.; Tommey, T. A.; Elles, C. G. Two-Photon Excitation of trans-Stilbene: Spectroscopy and Dynamics of Electronically Excited States above S_1. *J. Phys. Chem. B* **2015**, *119*, 9335.

(14) Kovalenko, S. A.; Dobryakov, A. L.; Ruthmann, J.; Ernsting, N. P. Femtosecond Spectroscopy of Condenced Phases with Chirped Supercontinuum Probing. *Phys. Rev. A: At., Mol., Opt. Phys.* **1999**, *59*, 2369−2384.

(15) Kovalenko, S. A.; Schanz, R.; Hennig, H.; Ernsting, N. P. Cooling Dynamics of an Optically Excited Molecular Probe in Solution from Femtosecond Broadband Transient Absorption Spectroscopy. *J. Chem. Phys.* **2001**, *115*, 3256−3273.

(16) Dobryakov, A. L.; Kovalenko, S. A.; Weigel, A.; Perez-Lustres, J. L.; Lange, J.; Müller, A.; Ernsting, N. P. Femtosecond Pump/Supercontinuum-probe Spectroscopy: Optimized Setup and Signal Analysis for Single-shot Spectral Referencing. *Rev. Sci. Instrum.* **2010**, *81*, 113106.

(17) Moreno, J.; Gerecke, M.; Grubert, L.; Kovalenko, S. A.; Hecht, S. Sensitized Two-Photon cis-trans Isomerization of a Thermally Stable *o*-Fluoroazobenzene, Manuscript in preparation.

(18) Knie, C.; Utecht, M.; Zhao, F.; Kulla, H.; Kovalenko, S.; Brouwer, A. M.; Saalfrank, P.; Hecht, S.; Bleger, D. orto-Fluoroazobenzenes: Visible Light Switches with Very Long-Lived Z Isomers. *Chem. - Eur. J.* **2014**, *20*, 16492−501.

(19) Mataga, N. *Molecular Interactions and Electronic Spectra*; Marcel Dekker Inc.: New York, 1970; p 385.

(20) Granovsky, A. A. Firefly, v. 8.1 http://classic.chem.msu.su/gran/firefly/index.html.

(21) Schmidt, M. W.; Baldridge, K. K.; Boatz, J. A.; Elbert, S. T.; Gordon, M. S.; Jensen, J. H.; Koseki, S.; Matsunaga, N.; Nguyen, K. A.; Su, S.; et al. General Atomic and Molecular Electronic Structure System. *J. Comput. Chem.* **1993**, *14*, 1347−1363 (see Supporting Information for the full reference).

(22) Frisch, M. J.; Trucks, G. W.; Schlegel, H. B.; Scuseria, G. E.; Robb, M. A.; Cheeseman, J. R.; Scalmani, G.; Barone, V.; Mennucci, B.; Petersson, G. A. et al. *Gaussian 09*, Revision A.02; Gaussian, Inc.: Wallingford CT, 2009. (see Supporting Information for the full reference).

(23) Moreno, J.; Dobryakov, A. L.; Ioffe, I. N.; Granovsky, A. A.; Hecht, S.; Kovalenko, S. A. Broadband Transient Absorption Spectroscopy with 1- and 2-Photon Excitation: Relaxation Paths and Cross-Sections of a Triphenylamine Dye in Solution. *J. Chem. Phys.* **2015**, *143*, 024311.

(24) Lakowicz, J. R. *Principles of Fluorescence Spectroscopy*; Springer: New York, 2011; Chapter 18.

(25) Kovalenko, S. A.; Dobryakov, A. L. On the Excitation Wavelength Dependence and Arrhenius Behavior of Stilbene Isomerization Rates in Solution. *Chem. Phys. Lett.* **2013**, *570*, 56−60.

(26) Kovalenko, S. A.; Dobryakov, A. L.; Ernsting, N. P. *Is Photoisomerization of Stilbene in Solution Directly Promoted by Solvent Collisions?* 2012, arXiv:1204.2142v2.

(27) Sadovnichy, V.; Tikhonravov, A.; Voevodin, V.; Opanasenko, A. "Lomonosov": Supercomputing at Moscow State University. In *Contemporary High Performance Computing*; CRC Press: Boca Raton, FL, 2013; pp 283−330.

DOI: 10.1021/acs.jpcb.5b07008
J. Phys. Chem. B 2015, 119, 12281−12288